



# Zero valent iron and goethite nanoparticles as new promising remediation techniques for As-polluted soils

D. Baragaño <sup>a</sup>, J. Alonso <sup>b</sup>, J.R. Gallego <sup>a,\*</sup>, M.C. Lobo <sup>b</sup>, M. Gil-Díaz <sup>b</sup>

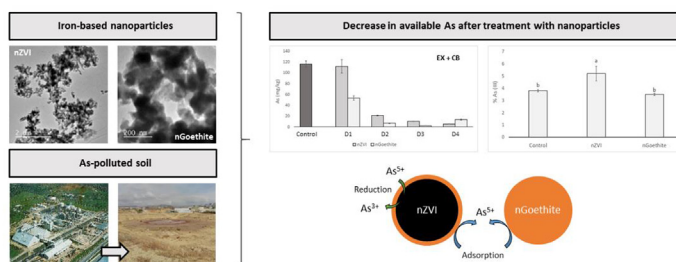
<sup>a</sup> INDUROT, Environmental Technology, Biotechnology, and Geochemistry Group, Universidad de Oviedo, Campus de Mieres, 33600 Mieres, Asturias, Spain

<sup>b</sup> IMIDRA, Instituto Madrileño de Investigación y Desarrollo Rural, Agrario y Alimentación, Finca "El Encín", Alcalá de Henares, 28800, Madrid, Spain

## HIGHLIGHTS

- NZVI and nGoethite immobilized As efficiently in a polluted soil.
- Doses higher than 1% of nGoethite caused phytotoxicity.
- Nanoparticle addition did not lead to a considerable increase in Fe availability.
- nGoethite emerges as an interesting alternative to nZVI for As immobilization.

## GRAPHICAL ABSTRACT



## ARTICLE INFO

### Article history:

Received 7 May 2019

Received in revised form

23 July 2019

Accepted 19 August 2019

Available online 22 August 2019

Handling Editor: Tsair-Fuh

### Keywords:

Arsenic

Soil pollution

nZVI

Goethite nanoparticles

Immobilization

Brownfield

## ABSTRACT

The capacity of two iron-based nanomaterials, namely goethite nanospheres (nGoethite) and zero valent iron nanoparticles (nZVI), to immobilize As in a polluted soil was evaluated and compared. The composition and morphology of the products were studied by energy dispersive X-ray analysis and transmission electron microscopy, while zeta potential and average sizes were determined by dynamic light scattering. To assess As immobilization, soil subsamples were treated with nGoethite or nZVI at a range of Fe doses (0.5%, 2%, 5% and 10%) and then studied by the TCLP test and the Tessier sequential extraction procedure. The influence of both nanoparticles on As speciation was determined, as was impact on soil pH, electrical conductivity, Fe availability and phytotoxicity (watercress germination). For nZVI, notable results were achieved at a dose of 2% (89.5% decrease in As, TCLP test), and no negative effects on soil parameters were detected. Indeed, even soil phytotoxicity was reduced and only at the highest dose was a slight increase in As<sup>3+</sup> detected. In contrast, excellent results were obtained for nGoethite at the lowest dose (0.2%) (82.5% decrease in As, TCLP test); however, soil phytotoxicity was increased at higher doses, probably due to a marked enhancement of electrical conductivity. For both types of nanoparticle, slight increases in Fe availability were observed. Thus, our results show that both nZVI and nGoethite have the capacity to effectively immobilize As in this brownfield. The use of lower doses of nGoethite emerges as a promising soil remediation strategy for soils affected by As pollution.

© 2019 Elsevier Ltd. All rights reserved.

## 1. Introduction

The closure of industrial and mining facilities has brought to light the presence of large volumes of contaminated soil worldwide (Adriano, 2001; Gallego et al., 2016; Santucci et al., 2018). These

\* Corresponding author.

E-mail address: [jgallego@uniovi.es](mailto:jgallego@uniovi.es) (J.R. Gallego).

sites, known as brownfields (Marker, 2018), are particularly common in areas with a history of heavy industrial activity. Among the pollutants found in brownfield soils, Potentially Toxic Elements (PTEs), such as Pb, As, Cu or Zn, are some of the most frequent due to their release during industrial processes (Lado et al., 2008; Magiera et al., 2018), atmospheric deposition (Boente et al., 2017; Davis and Birch, 2011; Gallego et al., 2013) and inappropriate dumping of waste (Alekseenko et al., 2018; Rao, 2014). PTEs, even at low concentrations, can pose a serious threat to human health and ecosystems (Fraga et al., 2005; Gopalakrishnan et al., 2015; Irem et al., 2019).

In particular, arsenic (As) is a highly toxic and carcinogenic element and as such it compromises ecosystem quality and human health (Hopkins et al., 2009). In general, As(V) and As(III) are the most common stable oxidation states of this heavy metal in soils (Aide et al., 2016), As(III) being more toxic than As(V). Classical methods for the remediation of As-contaminated soils require physical/chemical methods such as solidification/stabilization, soil washing, and electrokinetics, or biological strategies such as phytoremediation (Forján et al., 2016; González et al., 2019; Hasegawa et al., 2015; Khalid et al., 2017; Kumpiene et al., 2008; Mesa et al., 2017; Pérez-Sanz et al., 2013). Among the most common techniques used in situ, those based on arsenate immobilization through adsorption and surface complexation on iron-based compounds have been widely studied (Hartley et al., 2004; Hartley and Lepp, 2008; Chen and Li, 2010; Komárek et al., 2013). Sorption on iron oxides was found to lead to inner-sphere surface complexation, including monodentate, bidentate mononuclear, and bidentate binuclear complexes (Fendorf et al., 1997; Gao et al., 2006; Hua et al., 2012; Rahimi et al., 2015).

Recent years have witnessed the development of nano-remediation as a novel technique to immobilize heavy metal(oid)s, especially methods involving the addition of nanoscale zero valent iron nanoparticles (nZVI) to stabilize and reduce PTE availability (Gil-Díaz et al., 2017a, 2017b, 2019; Gonçalves, 2016; Mueller et al., 2012; O'Carroll et al., 2013). nZVI usually present acicular shapes, thus increasing the specific surface of granular iron and achieving higher reactivity due to their size (O'Carroll et al., 2013). Several studies have shown that nZVI effectively immobilize As in water samples and soils (Gil-Díaz et al., 2017a; Kim et al., 2012; Rahmani et al., 2010), even in field conditions (Gil-Díaz et al., 2019). In aqueous solutions, nZVI react with water and oxygen to form an outer Fe (hydr)oxide layer, so these particles present a core-shell structure (O'Carroll et al., 2013). In this context, differences in the structural properties of nZVI strongly influence the reactivity and aging of the particles (Fajardo et al., 2015; Gil-Díaz et al., 2017b, 2016a). In addition, risks due to the potential toxicity of nZVI have been reported and should be taken into account (Cagigal et al., 2018; Gil-Díaz and Lobo, 2018). In this regard, nanoparticle (NP) dose, exposure time, oxidation rate and Fe availability are parameters to be considered (Fajardo et al., 2012; Gil-Díaz et al., 2017b; Li et al., 2010; Saccà et al., 2014).

To overcome these difficulties, other NPs based on Fe oxides have been used for environmental remediation purposes. In this regard, they have shown greater stability than nZVI when used for PTE removal from water (Chen and Li, 2010; Rahimi et al., 2015) or even from soils (Waychunas et al., 2005; Zhang et al., 2010). In particular, iron oxy-hydroxide ( $\alpha$ -FeOOH) is a natural oxide mineral, known as goethite, which promotes contaminant sequestration (including As) by sorption processes (Giménez et al., 2007; Waychunas et al., 2005). Indeed, even synthetic goethite has been produced (Atkinson et al., 1968) and applied for As immobilization (O'Reilly et al., 2010). In this context, synthesized goethite have recently been used successfully to remove Cu and Pb from polluted

water, achieving better results than other iron oxides (Chen and Li, 2010; Rahimi et al., 2015). However, to the best of our knowledge, despite the great potential of goethite as an adsorbent, the capacity of goethite NPS (nGoethite) to remove As from water or immobilize As in soils has not been tested.

The main objectives of this work are: i) to compare the effectiveness of commercial nZVI and nGoethite to immobilize As in an industrial polluted soil; and ii) to determine potential toxic effects of these nanoparticles by means of Fe availability and soil phytotoxicity evaluation.

## 2. Materials and methods

### 2.1. Samples

Samples were taken from polluted soils in one of the main former fertilizer plants in southern Spain (Andalusia), which operated for almost forty years until its closure in 1997. Following its dismantling in 2001, characterization studies revealed areas with concentrations of As exceeding soil screening levels (Baragaño et al., 2018).

Within the area affected by As pollution, a 5-kg composite soil sample was collected from the surface layer (0–25 cm) with a manual auger. It was then air-dried, homogenized and sieved (<2 mm) prior to analysis.

### 2.2. Analyses

The physico-chemical properties of the soil were determined in representative subsamples using the Spanish official methodology (MAPA, 1994). In brief, organic matter was determined using the Walkley-Black method (dichromate oxidation); pH and electrical conductivity (EC) were measured in a 1:2.5 soil-to-water ratio; total nitrogen content was quantified by the Kjeldahl method; the percentage of carbonates was measured using a Bernard calcimeter; and available nutrients (Ca, K, Mg, Na) were extracted with 0.1 N ammonium acetate and quantified using a flame atomic absorption spectrometer (AA240FS, Varian). Grain size was characterized by wet-sieving and laser diffraction spectroscopy using the Aqueous Dry Module of an LS 13 320 MW system (Beckman Inc. Coulter).

Pseudo-total metal(loid) concentrations were determined after acid digestion with a mixture of 6 mL nitric acid (69% purity) and 2 mL of hydrochloric acid (37% purity), in a microwave reaction system (Multiwave Go, Anton Paar GmbH). In the digestion extract, the concentrations of Fe, Cd, Cr, Cu, Ni, Pb and Zn were quantified by flame atomic absorption spectrometry (FAAS) (AA240FS, Varian) and As by graphite furnace atomic absorption spectrometry (GFAAS) with Zeeman Correction (AA240Z, Varian).

### 2.3. Iron-based nanoparticles characterization

Two types of commercially iron NPs were purchased: Zero valent iron NPs (nZVI) called NANOFER 25S, obtained from Nano Iron s.r.o., (Rajhrad, Czech Republic), and goethite NPs (nGoethite) synthesized by Cerion Advanced Materials (USA) and obtained from Sigma-Aldrich (USA, #796093). The NPs were used immediately after receipt, thereby preventing any chemical alteration, and solutions were covered with aluminium foil to prevent light-induced degradation.

Chemical and macro-morphology studies of both types of NP were performed by scanning-electron microscope and energy dispersive X-ray spectroscopy (SEM-EDX) using a JEOL JSM-5600 Scanning Electron Microscope coupled to an Energy Dispersive X-ray analyzer (INCA Energy 200).

The size and morphology of the NPs were measured in a JEOL JEM-2100F transmission electron microscope (TEM). For TEM observations, sample preparation involved the dispersion of the NPs in a suspension of water by means of sonication, and deposition on a holey carbon film-coated copper grid and subsequent drying. The mean size of NPs was determined by image analysis and confirmed by dynamic light scattering (DLS) using a Zetasizer Nano ZS (Malvern Panalytical). Finally, to determine surface charge and given that the sorption mechanism between As and iron oxides is a surface phenomenon, the zeta potential of the NPs was determined using a Zetasizer Nano ZS.

#### 2.4. Batch experiments and monitoring

To test the effectiveness of the NPs for As immobilization, 20-g subsamples of polluted soil were treated with each type of NP at different doses in 50-mL plastic vials. nZVI doses of 0.5%, 2%, 5% and 10% (w:w) were selected on the basis of previous studies with other As-polluted soils (Gil-Díaz et al., 2017a, 2017b; 2016a). nGoethite doses of 0.2%, 1%, 2% and 5% were selected in order to facilitate comparison of the effects of the two distinct types of NPs at a similar Fe content per gram of soil, i.e., the amount of Fe added to the soil corresponded to that of the nZVI experiments. Therefore increasing doses of Fe are labeled henceforth as D1, D2, D3 and D4 irrespective of the NPs used.

Before beginning the experiments, deionized water was added to the soil samples to achieve water holding capacity in order to improve nanoparticles and soil contact. NPs were then applied, except for control tests, which were treated only with deionized water. Experiments were carried out in triplicate. Vials were shaken for 72 h at 100 rpm in a Reax 2 shaker (Heidolph Instrument GmbH & Co. KG). After shaking, samples were air dried.

To quantify potential As leachability, the TCLP test (Toxicity Characteristic Leaching Procedure) was performed following the USEPA Method 1311 (1992). Furthermore, to determine the potential mobility and availability of As in soil samples, the sequential extraction procedure proposed by Tessier et al. (1979) was also performed. In brief, extracts with reagents of increasing strengths were sequentially added to the subsamples. The following fractions were obtained: exchangeable (EX); bound to carbonates (CB); bound to Fe–Mn oxides (OX); bound to organic matter (OM); and residual (RS). As and Fe concentrations were measured in the extracts following the methodology described in section 2.2. Electrical conductivity (EC) and pH were also measured to evaluate the influence of NP application on soil properties in a suspension of soil and distilled water (1:2.5).

For measuring As species, 0.1 g of soil and 15 mL of the extracting agent (1 M  $\text{H}_3\text{PO}_4$  + 0.1 M ascorbic acid) were placed in a microwave vessel and digested (Multiwave 3000, Anton Paar GmbH) at 60 W for 10 min (García-Manyes et al., 2002). After cooling, the extracts were diluted and filtered (0.45  $\mu\text{m}$ ). The As species were separated in a 4.6 mm  $\times$  150 mm As Separation Column (Agilent Technologies) fitted to a 1260 Infinity HPLC coupled to a 7700 ICP-MS (Agilent Technologies) using a mobile phase of 2 M PBS (Phosphate Buffered Saline)/0.2 M EDTA (pH = 6.0) at a flow of 1 mL/min.

#### 2.5. Soil phytotoxicity

The phytotoxicity of the NP-treated and untreated soil samples was determined using a modified version of the Zucconi test (Zucconi et al., 1985), as described in a previous study (Gil-Díaz et al., 2014). In brief, six watercress (*Nasturtium officinale*) seeds moistened with 6 mL of distilled water (control) or soil extract were placed in triplicate Petri dishes. Soil extracts were obtained by

means of 5 g of air-dried in contact with 50 mL of distilled water at 60 °C during 30 min, followed by filtering with a Whatman paper (541 grade). After two days of incubation in the dark at 26–27 °C, the seed germination percentage was calculated and the root length of seedlings was measured. The germination index (GI) was calculated as follows:  $\text{GI} (\%) = G \text{ Ls}/\text{Lc}$ , where G is the percentage of germination obtained with respect to the control values, Ls is the mean root length in the soil extracts, and Lc is the mean root length in the control.

#### 2.6. Statistical analysis

Data were statistically treated using version 24.0 of the SPSS program for Windows. Analysis of variance (ANOVA) and test of homogeneity of variance were carried out. In the case of homogeneity ( $p < 0.05$ ), a post hoc least significant difference (LSD) test was carried out. If there was no homogeneity, Dunnett's T3 test was performed.

### 3. Results and discussion

#### 3.1. Soil characterization

The initial soil properties are shown in Table S1 (Supplementary Material). Results revealed typical characteristics of soils in arid areas, i.e. low organic matter and nitrogen content, alkaline pH and a high carbonate content. The texture was sandy loam. The mean concentrations of Cu, Ni, Pb, Zn, Cr, and Cd were below the current Regional Screening Levels for industrial uses (BOJA and Boletín Oficial de la Junta de Andalucía, 38, February 2015). In contrast, the concentration of As was 30 times more than the maximum permitted levels.

#### 3.2. Nanoparticle characterization

In brief, the NANOFER 25S slurry is an aqueous dispersion of stabilized nZVI. According to the commercial specification, its Fe(0) content is 14–18%, and 2–6% of magnetite is also present, the average size of the NPs is around 60 nm, the suspension is strongly alkaline (pH 11–12), and the active surface area is 20  $\text{m}^2/\text{g}$  (additional details are available at [www.nanoiron.cz](http://www.nanoiron.cz)).

In contrast, nGoethite are iron oxy-hydroxide ( $\alpha$ -FeOOH) NPs dispersed in an aqueous solution. Trace metal analysis revealed low concentrations (total concentration lower than 208 ppm) of Ag, Al, Ba, Cd, Cr, Mg, Pb, Ti, W and Zn and a pH of 3.2 when in suspension, according to the product's certificate of analysis.

Although nZVI (NANOFER 25s) have been previously described (Klimkova et al., 2011; Laumann et al., 2013; Schmid et al., 2015), to extend knowledge about nGoethite and compare the two types of NPs, additional analyses were carried out prior to the batch experiments. SEM images of nZVI revealed a surface topography (Fig. S1A, Supplementary Material) formed by spheres of regular sizes. However, SEM images of nGoethite (Fig. S1B, Supplementary Material) showed a product with a blade shape. Regarding the chemical composition of nZVI (Fig. S1C, Supplementary Material) and nGoethite (Fig. S1D, Supplementary Material), Fe was found to be the predominant element in the former (more than 80% Fe), and a certain degree of oxidation was observed (less than 20% O). In contrast, iron oxides were the main components of nGoethite (only 60% Fe). Minor components were observed, such as Si and C, which are related to the sample carrier composition.

TEM images of nZVI (Fig. 1A and C) and nGoethite (Fig. 1B and D) showed that the NPs were not well distributed, probably due to the drying step carried out in the TEM sample preparation. Therefore, DLS analysis was preferred in order to determine the nanoparticles



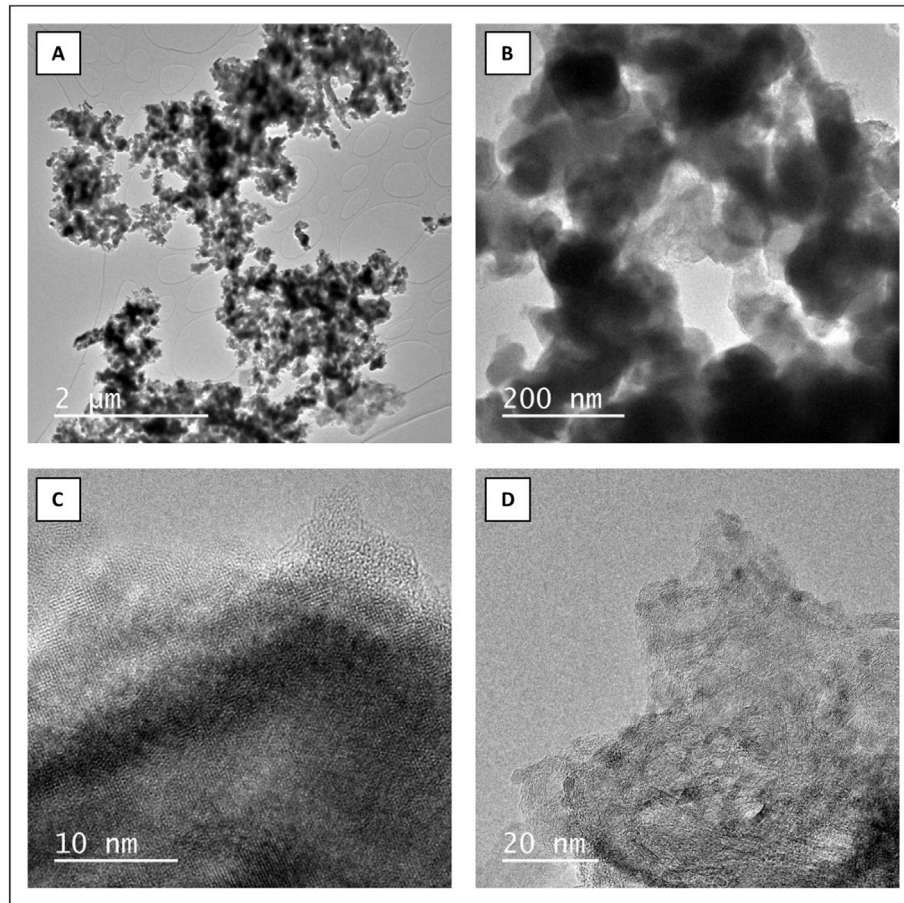


Fig. 1. TEM pictures (A and C: nZVI; B and D: nGoethite) of iron nanoparticles.

size. Regarding nZVI, the analysis revealed a diameter close to 60 nm which is consistent with the commercial specification, whereas the average diameter of nGoethite was close to 2.7 nm. Comparing size of nanoparticles distribution of both types, nGoethite are one order of magnitude lower and the distribution is narrower than nZVI (Fig. S2).

The zeta potential of nZVI was  $-31.9$  mV, a value that is attributed to the polyacrylic acid (PAA) coating used to stabilize the particles, thereby preventing agglomeration caused by counter attractive magnetic and van der Waals forces (Laumann et al., 2013). In contrast, the charge of nGoethite was 86 mV, a positive value consistent with the low pH of the suspension (Giménez et al., 2007).

### 3.3. Batch experiment evaluation

#### 3.3.1. Impact on As availability

The two NP treatments significantly reduced As leachability at the four doses applied, as shown by the TCLP test (Fig. 2). Generally, high As immobilization percentages (80–99%) were found in most of the doses, except for D1 of nZVI. However, generally speaking, nGoethite showed greater As immobilization yields (82.5%, 99.3%, 99.7% and 99.8% at increasing doses) than nZVI (41.6%, 89.5%, 96.2% and 97.6%).

For all the Tessier fractions (Tessier et al., 1979), a common pattern of As distribution, irrespective of the doses of NPs used, was observed (Fig. 3), namely the RS fraction increased, while the other fractions decreased. Only in the case of the lowest dose of nZVI was

a significant effect not detected. In this regard, previous studies using nZVI also reported a significant increase in As associated with the RS fraction (Gil-Díaz et al., 2014; 2016a,b, 2017a; 2017b).

Specifically, the concentration of As in the EX fraction was reduced after the treatment with nZVI at doses D2, D3 and D4 (a reduction ranging from 74% to 94% was observed). In the case of nGoethite, the As concentration in this fraction was reduced at all doses—53% at the lowest dose and up to 99% at the highest. Thus, nGoethite at the lowest dose resulted significantly more efficient than nZVI at reducing the As concentration in the most available fraction. In the CB fraction, As concentration was only significantly reduced at D2, D3 and D4 using nZVI, observing a reduction of between 86% and 96%. In contrast, nGoethite at the lowest dose caused the concentration of As in the CB fraction to fall by 54%, while at higher doses, D2 and D3, it reduced the concentration of this heavy metal in this fraction by up to 92% and 97% respectively. However, at the highest dose, D4, the reduction fell to 82%. This decrease in effectiveness might be due to the agglomeration of the NPs at such a high dosage or by some other effect related to the pH, EC and Fe availability of the soil (Gil-Díaz and Lobo, 2018; Singh and Misra, 2015). A similar decrease in As concentration to that observed in the most available fractions was detected in the less mobile OX and OM fractions. Treatment with nZVI, except at the lowest dose tested, led to a reduction in the OX and OM fractions, observing 50–90% and 79–99% decreases, respectively. nGoethite at all the doses tested led to significant reductions in the OX and OM fractions, with decreases of 31–99% and 49–99.9%, respectively. Finally, the concentration of As in the RS fraction, the non-

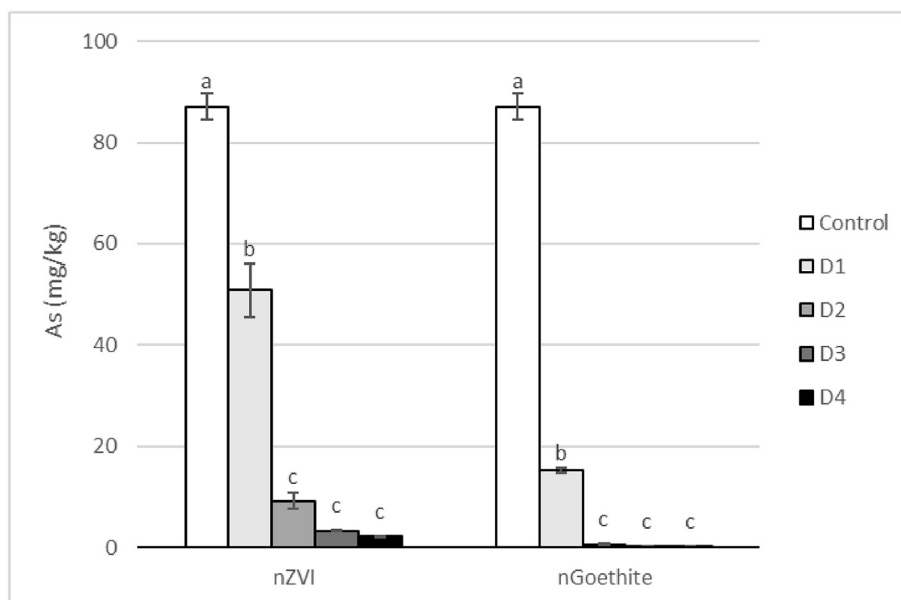


Fig. 2. Mean concentration of arsenic (mg/kg) in TCLP extracts. For each type of nanoparticle, bars with the same letter do not differ significantly ( $p < 0.05$ ).

available one, was significantly increased after treatment with both types of NP at all doses, especially at the highest dose.

The reactivity and effectiveness of NPs for metal(oid) immobilization depend on the properties of the NPs (e.g. size, coating, composition, surface charge) and soil conditions (Gil-Díaz et al., 2017a). Regarding nZVI, this nanomaterial immobilizes As by adsorption onto iron oxides in the shell surrounding the Fe(0) through inner-sphere surface complexation (Gil-Díaz et al., 2017a, 2014). Nevertheless, the surface chemistry of goethite differs to that of ZVI and varies with pH. At low pH, the hydroxyl groups at the surface of goethite are doubly protonated ( $\equiv\text{FeOH}_2^+$ ) and the surface charge is thus positive (Giménez et al., 2007; O'Reilly et al., 2010), which is consistent with the positive zeta potential value determined in the nGoethite characterization. At these acidic pH values, the electrostatic attraction between the negative oxoanions and the positive charge of the NPs favors adsorption (Siddiqui and Chaudhry, 2018). Therefore, the lower size of nGoethite NPs compared to nZVI, their corresponding higher specific surface, and adequate surface charge may explain the greater As immobilization achieved.

The results show that the application of Fe-based NPs, nZVI and nGoethite, to this industrial brownfield site significantly reduced the availability of As in the soil, as revealed by the TCLP test and the Tessier method. The effectiveness of the As immobilization depends on the dose of NPs used, although doses of nZVI higher than 5%, as seen in previous studies (Gil-Díaz et al., 2017a, 2016a, 2014), and 1% of nGoethite did not show higher efficiency. The best stabilization results were obtained with nGoethite, even at the lowest dose tested (0.2%). The As immobilization capacity of this nanomaterial at such a low dose is a critical factor when considering field-scale remediation.

### 3.3.2. Impact on As speciation

The As speciation analysis in the original soil revealed that the predominant form of As (>96%) was arsenate ( $\text{As}^{5+}$ ), whereas arsenite ( $\text{As}^{3+}$ ) was below 4%. The reduction of  $\text{As}^{5+}$  to  $\text{As}^{3+}$  species by nZVI was reported by Ramos et al. 2009) in water samples under anaerobic conditions, although in previous studies with As-polluted soils (Gil-Díaz et al., 2017a, 2016a, 2014), this reduction

was not been detected. In our case, the addition of nZVI at the highest dose caused a minor but significant increase of 1.4% in  $\text{As}^{3+}$  (arsenite) proportion, a more mobile and phytotoxic form compared to  $\text{As}^{5+}$  (arsenate) (Table 1). Nevertheless, as shown above, As immobilization by adsorption onto iron oxides in the outer layer of the NPs reduced As availability, as measured by the TCLP test and Tessier extracts. Therefore, the main process involved in the immobilization of As was arsenate adsorption, although a reduction process was also present but to a minor extent, which can be explained by the core-shell structure of nZVI. On the other hand, the reduction mechanism was not observed when nGoethite was tested; i.e., no changes in speciation were observed (Table 1). This observation points to an additional advantage of nGoethite over nZVI under the experimental conditions tested.

### 3.3.3. Impact on the pH and EC of soil

Given the different chemical nature of the two types of NPs applied and the differences of pH in the suspensions (the nZVI suspension was alkaline, while the nGoethite suspension was acidic), we examined their effects at a range of dosages on soil pH and EC.

The data are shown in Table 2. The application of nZVI did not affect pH or EC at any of the doses tested. However, nGoethite addition at the highest dose led to a significant decrease of pH, falling from 8.23 to 7.38. A lower pH enhances As immobilization. In relation to EC soil values, nGoethite induced a notable increase, ranging from  $0.55 \text{ dS m}^{-1}$  at the lowest dose to  $5.38 \text{ dS m}^{-1}$  at the highest one. This increase should be taken into account from the point of view of soil functionality, as the highest dose (D4) will impair the biological activity of the soil and plant development. As immobilization was almost completed at moderate doses, thus it is suggested that the notable EC increase in doses D3 and especially in D4, is probably caused by an excess of nGoethite nanoparticles.

### 3.3.4. Impact on Fe availability

To determine the quantitative impact of the NP treatments on the availability of Fe in the soil, Fe concentration was measured. The Fe distribution in the TCLP extracts and in the most available Tessier fractions are showed in Fig. 4.

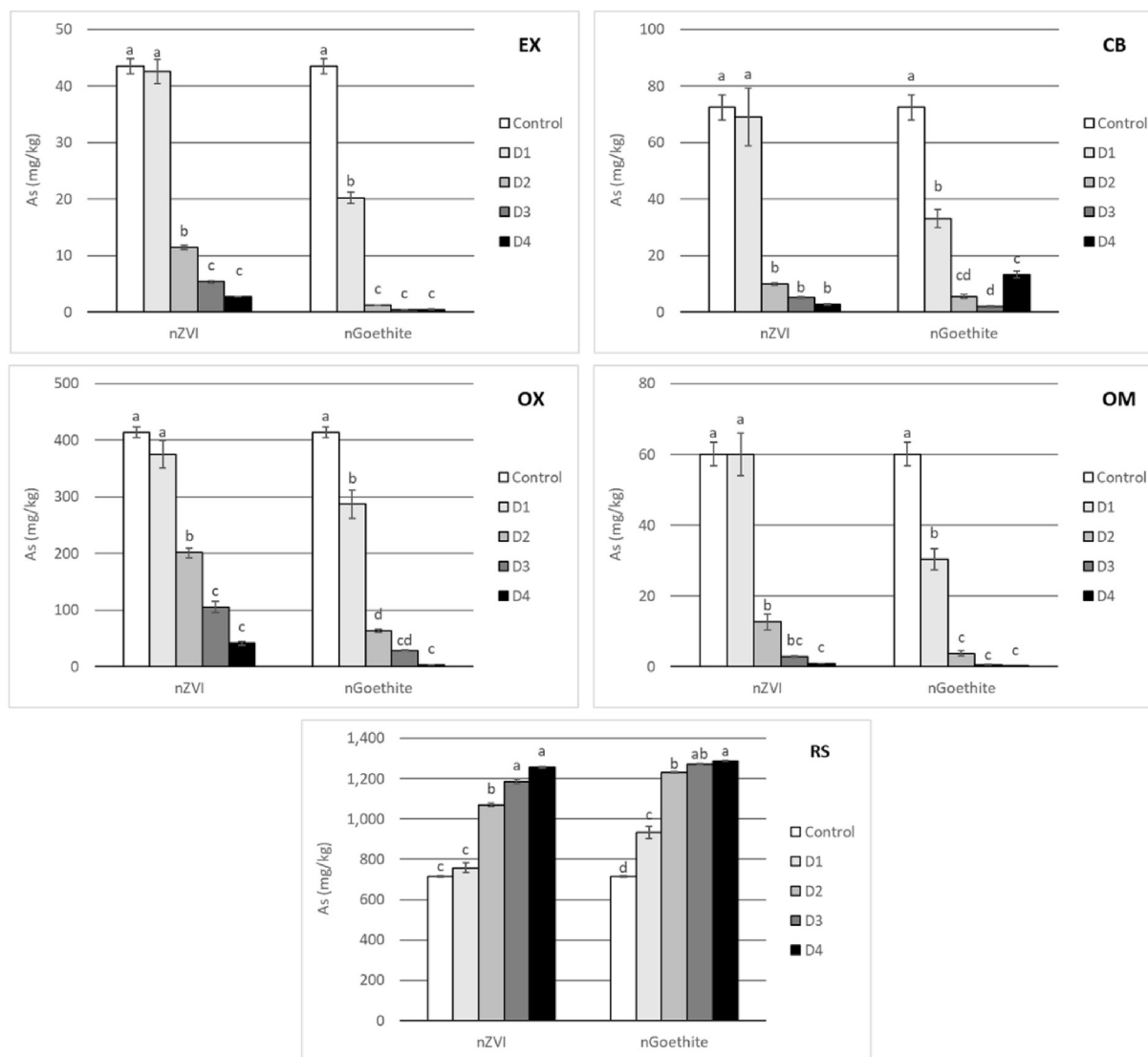


**Fig. 3.** Mean concentration of arsenic (mg/kg) in EX (exchangeable), CB (bound to carbonates), OX (bound to Fe–Mn oxides), OM (bound to organic matter) and RS (residual) soil fractions. For each type of nanoparticle, bars with the same letter do not differ significantly ( $p < 0.05$ ).

**Table 1**

Arsenic speciation results for untreated samples and samples treated at the highest dose (D4). For each type of nanoparticle, data with the same letter do not differ significantly ( $p < 0.05$ ). Note that mass recovery of the digestion method used is approximately 25% below of that obtained with aqua regia digestion.

Sample	As(III)	As(V)
Control	3.8 ± 0.1a	96.2 ± 0.1a
nZVI	5.2 ± 0.6b	94.8 ± 0.6b
nGoethite	3.5 ± 0.1a	96.5 ± 0.1a

The TCLP tests showed a slight increase in available Fe in all the treatments compared with untreated soil. The increase was not dose-dependent.

Regarding the most available Tessier fractions, the addition of both types of NPs revealed a different behavior.

The concentration of Fe in the EX fraction did not show significant variations for either type of NP, with the exception of nGoethite treatment at the highest dose, which caused an increase of 42%. This increase could be due to the extremely high dose; i.e., the Fe that has not reacted with As and other soil components is in an

**Table 2**

Mean values and standard deviation of pH and electrical conductivity of soil samples treated with nZVI and nGoethite nanoparticles. For each type of nanoparticle, data with the same letter do not differ significantly ( $p < 0.05$ ).

Treatment	Dose	pH	EC (dS/m)
Control	0%	8.23 ± 0.04a	0.28 ± 0.01a
nZVI	D1	8.58 ± 0.10a	0.26 ± 0.01a
	D2	8.48 ± 0.09a	0.30 ± 0.01a
	D3	8.63 ± 0.11a	0.37 ± 0.01b
	D4	9.05 ± 0.20a	0.46 ± 0.01c
nGoethite	D1	8.02 ± 0.03 ab	0.55 ± 0.01b
	D2	8.00 ± 0.09 ab	1.56 ± 0.02c
	D3	8.56 ± 0.11a	2.43 ± 0.07d
	D4	7.38 ± 0.09b	5.38 ± 0.03e

available form.

In the CB fraction, Fe concentration increased between 430% and –856% in the nZVI treatment at D2, D3 and D4. In the case of nGoethite treatment, no variation was observed in the CB fraction, with the exception of the highest dose, in which a marked increase was detected, probably attributable to the same reason as the

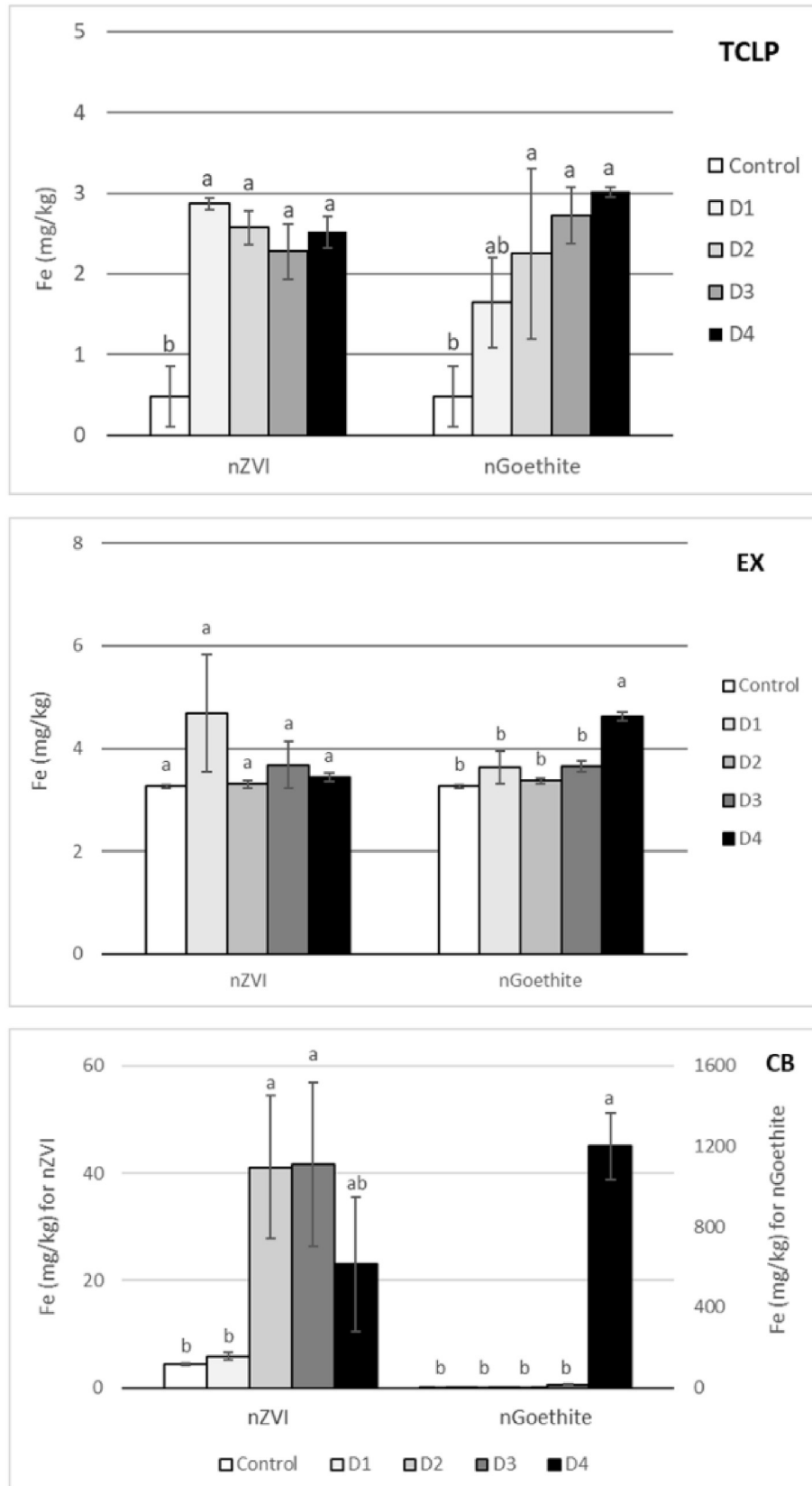


**Fig. 4.** Average concentration of iron (mg/kg) in TCLP extracts and in the EX (exchangeable) and CB (bound to carbonates) soil fractions of the Tessier procedure. For each type of nanoparticle, bars with the same letter do not differ significantly ( $p < 0.05$ ).

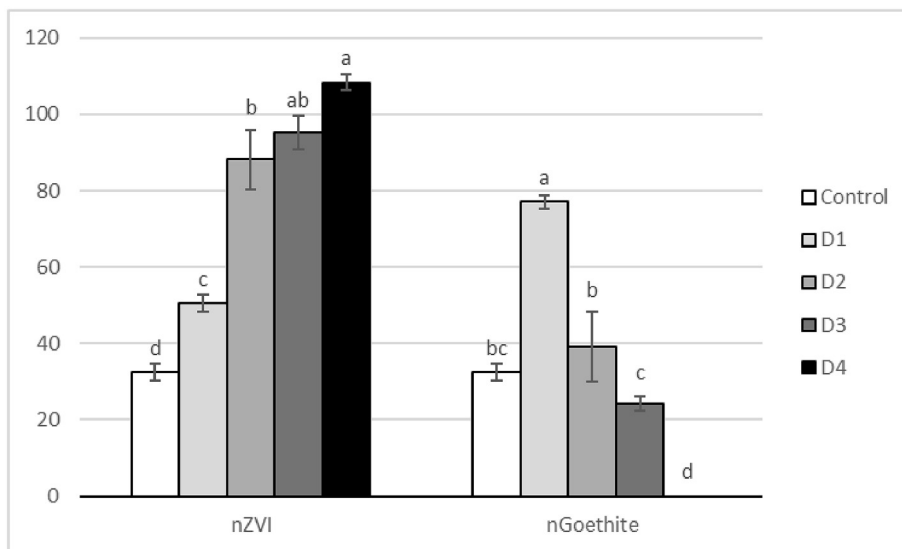


**Fig. 5.** Mean germination index (%) of watercress for the soils treated with different doses of nanoparticles. For each type of nanoparticle, bars with the same letter do not differ significantly ( $p < 0.05$ ).

increase in the EX fraction referred to above.

In summary, Fe is normally associated with the non-available fractions of Tessier extracts (Gil-Díaz et al., 2016a, 2014). Therefore, in this case, it is particularly relevant that very small differences and very low increases in Fe availability were observed for low doses of both nZVI and nGoethite. However, medium and high doses of nZVI and the highest dose of nGoethite led to a notable increase in the Fe bound to the CB fraction, and also to the EX fraction for nGoethite.

### 3.3.5. Soil phytotoxicity

The results of the phytotoxicity assay are shown in Fig. 5. According to Zucconi et al. (1985), GI values below 50% indicate high phytotoxicity, between 50% and 80% moderate phytotoxicity, and above 80% no phytotoxicity.

Initially, the untreated soil was highly phytotoxic to watercress since the GI of these plants was  $< 50\%$ . The application of nZVI at all the doses tested significantly reduced phytotoxicity. These results are consistent with those obtained from the sequential extraction procedure and TCLP tests, which showed that treated soils showed a lower availability of As, the only contaminant in the soil. The same effect was observed with the lowest dose of nGoethite, but not with the higher ones. The latter observation can be explained by the dramatic increase in soil EC when high amounts of nGoethite are added, as described above.

## 4. Conclusions

The application of nZVI and nGoethite to soil samples from a brownfield polluted with As caused a marked reduction in the availability of this heavy metalloid. The effectiveness of the immobilization was significantly higher for nGoethite. However, the marked effect of high doses of this nGoethite on the EC and phytotoxicity of soil may limit the use of this nanomaterial for remediation purposes. The highest dose of nZVI (10% w/w) tested was observed to cause a slight increase in arsenate reduction to arsenite (lower than 2%).

Our results demonstrate that both nZVI and nGoethite, at the lowest doses assayed (0.5% and 0.2%, respectively) are efficient, although the former showed poorer As immobilization yields, as

revealed by measurements of As availability in the EX and CB fractions of the Tessier method and in TCLP extracts. Moderate doses of nZVI outperformed nGoethite with respect to As immobilization.

On the basis of our findings, we conclude that, at the lowest dose assayed (0.2%), nGoethite is a safe and promising technique for As immobilization. Regarding nZVI, a dose of 2% would show a similar result for the remediation of the brownfield. Pilot or real-scale studies are now required to validate these conclusions in a range of soil types.

## Acknowledgments

This work was supported by the research projects REHABILITACIÓN 2016-78222-C2-1-R (AEI/FEDER, UE), FP-16-NANOREMED (IMIDRA, Comunidad de Madrid, Spain), and CTM 2016-75894-P (MINECO).

We would like also to thank the Environmental Assay Unit and the Electronic Microscope of the Scientific and Technical Services of the University of Oviedo for technical support. Diego Baragaño obtained a grant from the “Formación del Profesorado Universitario” program, financed by the “Ministerio de Educación, Cultura y Deporte de España”.

## Appendix A. Supplementary data

Supplementary data to this article can be found online at <https://doi.org/10.1016/j.chemosphere.2019.124624>.

## References

- Adriano, D.C., 2001. Trace Elements in Terrestrial Environments Biogeochemistry, Bioavailability, and Risks of Metals, ume I. <https://doi.org/10.1007/978-0-387-21510-5>.
- Aide, M., Beighley, D., Dunn, D., 2016. Arsenic in the soil Environment: a soil chemistry review. *Int. J. Appl. Agric. Res.* 11, 1–28.
- Alekseenko, V.A., Bech, J., Alekseenko, A.V., Shvydkaya, N.V., Roca, N., 2018. Environmental impact of disposal of coal mining wastes on soils and plants in Rostov Oblast, Russia. *J. Geochem. Explor.* 184, 261–270. <https://doi.org/10.1016/j.gexplo.2017.06.003>.
- Atkinson, R.J., Posner, A.M., Quirk, J.P., 1968. Crystal nucleation in Fe(III) solutions and hydroxide gels. *J. Inorg. Nucl. Chem.* 30, 2371–2381. [https://doi.org/10.1016/0022-1902\(68\)80247-7](https://doi.org/10.1016/0022-1902(68)80247-7).



- Baragaño, D., Rodríguez-Valdés, E., Peláez, A.I., Boente, C., Matanzas, N., García, N., Gallego, J.L.R., 2018. Environmental forensic study and remediation feasibility in an abandoned industrial site. *Proceedings* 2, 1503. In: <https://doi.org/10.3390/proceedings2231503>.
- Boente, C., Matanzas, N., García-González, N., Rodríguez-Valdés, E., Gallego, J.R., 2017. Trace elements of concern affecting urban agriculture in industrialized areas: a multivariate approach. *Chemosphere* 183, 546–556. <https://doi.org/10.1016/j.chemosphere.2017.05.129>.
- BOJA, Boletín Oficial de la Junta de Andalucía, 38, February 2015. Regulation that regulates the regime applicable to contaminated soils. [https://www.juntadeandalucia.es/medioambiente/portal\\_web/web/temas\\_ambientales/suelo/suelos\\_contaminados/reglamento\\_suelos\\_contaminados.pdf](https://www.juntadeandalucia.es/medioambiente/portal_web/web/temas_ambientales/suelo/suelos_contaminados/reglamento_suelos_contaminados.pdf). (Accessed February 2019).
- Cagigal, E., Ocejó, M., Gallego, J.R., Peláez, A.I., Rodríguez-Valdés, E., 2018. Environmental effects of the application of iron nanoparticles for site remediation. In: *Iron Nanomaterials for Water and Soil Treatment*, pp. 283–307. <https://doi.org/10.1201/b22501-12>.
- Chen, Y.H., Li, F.A., 2010. Kinetic study on removal of copper(II) using goethite and hematite nano-photocatalysts. *J. Colloid Interface Sci.* 347, 277–281. <https://doi.org/10.1016/j.jcis.2010.03.050>.
- Davis, B.S., Birch, G.F., 2011. Spatial distribution of bulk atmospheric deposition of heavy metals in metropolitan Sydney, Australia. *Water, Air, Soil Pollut* 214, 147–162. <https://doi.org/10.1007/s11270-010-0411-3>.
- Fajardo, C., Ortiz, L.T., Rodríguez-Membibre, M.L., Nande, M., Lobo, M.C., Martín, M., 2012. Assessing the impact of zero-valent iron (ZVI) nanotechnology on soil microbial structure and functionality: a molecular approach. *Chemosphere* 86, 802–808. <https://doi.org/10.1016/j.chemosphere.2011.11.041>.
- Fajardo, C., Gil-Díaz, M., Costa, G., Alonso, J., Guerrero, A.M., Nande, M., Lobo, M.C., Martín, M., 2015. Residual impact of aged nZVI on heavy metal-polluted soils. *Sci. Total Environ.* 535, 79–84. <https://doi.org/10.1016/j.scitotenv.2015.03.067>.
- Fendorf, S., Eick, M.J., Grossl, P., Sparks, D.L., 1997. Arsenate and chromate retention mechanisms on goethite. 1. Surface structure. *Environ. Sci. Technol.* 31, 315–320. <https://doi.org/10.1021/es950653t>.
- Forján, R., Asensio, V., Rodríguez-Vila, A., Covelo, E.F., 2016. Contribution of waste and biochar amendment to the sorption of metals in a copper mine tailing. *Catena* 137, 120–125. <https://doi.org/10.1016/j.catena.2015.09.010>.
- Fraga, C.G., Oteiza, P.I., Keen, C.L., 2005. Trace elements and human health. *Mol. Asp. Med.* 26, 233–234. <https://doi.org/10.1016/j.mam.2005.07.014>.
- Gallego, J.R., Ortiz, J.E., Sierra, C., Torres, T., Llamas, J.F., 2013. Multivariate study of trace element distribution in the geological record of Roñanzas Peat Bog (Asturias, N. Spain). *Paleoenvironmental evolution and human activities over the last 8000calyr BP*. *Sci. Total Environ.* 454–455, 16–29. <https://doi.org/10.1016/j.scitotenv.2013.02.083>.
- Gallego, J.R., Rodríguez-Valdés, E., Esquinas, N., Fernández-Braña, A., Affé, E., 2016. Insights into a 20-ha multi-contaminated brownfield megasite: an environmental forensics approach. *Sci. Total Environ.* 563–564, 683–692. <https://doi.org/10.1016/j.scitotenv.2015.09.153>.
- Gao, S., Goldberg, S., Herbel, M.J., Chalmers, A.T., Fujii, R., Tanji, K.K., 2006. Sorption processes affecting arsenic solubility in oxidized surface sediments from Tulare Lake Bed, California. *Chem. Geol.* 228, 33–43. <https://doi.org/10.1016/j.chemgeo.2005.11.017>.
- García-Manyes, S., Jiménez, G., Padró, A., Rubio, R., Rauret, G., 2002. Arsenic speciation in contaminated soils. *Talanta* 58, 97–109. [https://doi.org/10.1016/S0039-9140\(02\)00259-X](https://doi.org/10.1016/S0039-9140(02)00259-X).
- Gil-Díaz, M., Lobo, M.C., 2018. In: Faisal, M., et al. (Eds.), *Phytotoxicity of Nanoscale Zerovalent Iron (nZVI) in Remediation Strategies in: Phytotoxicity of Nanoparticles*. Springer International Publishing AG, part of Springer Nature 2018. [https://doi.org/10.1007/978-3-319-76708-6\\_13](https://doi.org/10.1007/978-3-319-76708-6_13).
- Gil-Díaz, M., Alonso, J., Rodríguez-Valdés, E., Pinilla, P., Lobo, M.C., 2014. Reducing the mobility of arsenic in brownfield soil using stabilised zero-valent iron nanoparticles. *J. Environ. Sci. Heal. - Part A Toxic/Hazardous Subst. Environ. Eng.* 49, 1361–1369. <https://doi.org/10.1080/10934529.2014.928248>.
- Gil-Díaz, M., Díez-Pascual, S., González, A., Alonso, J., Rodríguez-Valdés, E., Gallego, J.R., Lobo, M.C., 2016a. A nanoremediation strategy for the recovery of an As-polluted soil. *Chemosphere* 149, 137–145. <https://doi.org/10.1016/j.chemosphere.2016.01.106>.
- Gil-Díaz, M., González, A., Alonso, J., Lobo, M.C., 2016b. Evaluation of the stability of a nanoremediation strategy using barley plants. *J. Environ. Manag.* 165, 150–158. <https://doi.org/10.1016/j.jenvman.2015.09.032>.
- Gil-Díaz, M., Alonso, J., Rodríguez-Valdés, E., Gallego, J.R., Lobo, M.C., 2017a. Comparing different commercial zero valent iron nanoparticles to immobilize As and Hg in brownfield soil. *Sci. Total Environ.* 584–585, 1324–1332. <https://doi.org/10.1016/j.scitotenv.2017.02.011>.
- Gil-Díaz, M., Pinilla, P., Alonso, J., Lobo, M.C., 2017b. Viability of a nanoremediation process in single or multi-metal(loid) contaminated soils. *J. Hazard Mater.* 321, 812–819. <https://doi.org/10.1016/j.jhazmat.2016.09.071>.
- Gil-Díaz, M., Rodríguez-Valdés, E., Alonso, J., Baragaño, D., Gallego, J.R., Lobo, M.C., 2019. Nanoremediation and long-term monitoring of brownfield soil highly polluted with As and Hg. *Sci. Total Environ.* 675, 165–175. <https://doi.org/10.1016/j.scitotenv.2019.04.183>.
- Giménez, J., Martínez, M., de Pablo, J., Rovira, M., Duro, L., 2007. Arsenic sorption onto natural hematite, magnetite, and goethite. *J. Hazard Mater.* 141, 575–580. <https://doi.org/10.1016/j.jhazmat.2006.07.020>.
- González, A., García-Gonzalo, P., Gil-Díaz, M., Alonso, J., Lobo, M.C., 2019. Compost-assisted phytoremediation of As-polluted soil. *J. Soils Sediments*. <https://doi.org/10.1007/s11368-019-02284-9>.
- Gonçalves, J.R., 2016. The soil and groundwater remediation with zero valent iron nanoparticles. In: *Procedia Engineering*, pp. 1268–1275. <https://doi.org/10.1016/j.proeng.2016.06.122>.
- Gopalakrishnan, A., Krishnan, R., Thangavel, S., Venugopal, G., Kim, S.J., 2015. Removal of heavy metal ions from pharma-effluents using graphene-oxide nanosorbents and study of their adsorption kinetics. *J. Ind. Eng. Chem.* 30, 14–19. <https://doi.org/10.1016/j.jiec.2015.06.005>.
- Hartley, W., Lepp, N.W., 2008. Remediation of arsenic contaminated soils by iron-oxide application, evaluated in terms of plant productivity, arsenic and phytotoxic metal uptake. *Sci. Total Environ.* 390, 35–44. <https://doi.org/10.1016/j.scitotenv.2007.09.021>.
- Hartley, W., Edwards, R., Lepp, N.W., 2004. Arsenic and heavy metal mobility in iron oxide-amended contaminated soils as evaluated by short- and long-term leaching tests. *Environ. Pollut.* 131, 495–504. <https://doi.org/10.1016/j.envpol.2004.02.017>.
- Hasegawa, H., Rahman, I.M.M., Rahman, M.A., 2015. Environmental remediation technologies for metal-contaminated soils. *Environmental Remediation Technologies for Metal-Contaminated Soils*. <https://doi.org/10.1007/978-4-431-55759-3>.
- Hopkins, J., Watts, P., Hosford, M., 2009. Contaminants in soil: updated collation of toxicological data and intake values for humans Inorganic arsenic. Science report: SC050021/TOX 1. Environment Agency. <http://webarchive.nationalarchives.gov.uk/20140328084622/http://www.environment-agency.gov.uk/research/planning/64002.aspx>. (Accessed February 2019).
- Hua, M., Zhang, S., Pan, B., Zhang, W., Lv, L., Zhang, Q., 2012. Heavy metal removal from water/wastewater by nanosized metal oxides: a review. *J. Hazard Mater.* <https://doi.org/10.1016/j.jhazmat.2011.10.016>.
- Irem, S., Islam, E., Maathuis, F.J.M., Niazi, N.K., Li, T., 2019. Assessment of potential dietary toxicity and arsenic accumulation in two contrasting rice genotypes: effect of soil amendments. *Chemosphere* 225, 104–114. <https://doi.org/10.1016/j.chemosphere.2019.02.202>.
- Khalid, S., Shahid, M., Niazi, N.K., Murtaza, B., Bibi, I., Dumat, C., 2017. A comparison of technologies for remediation of heavy metal contaminated soils. *J. Geochem. Explor.* 182, 247–268. <https://doi.org/10.1016/j.gexplo.2016.11.021>.
- Kim, K.R., Lee, B.T., Kim, K.W., 2012. Arsenic stabilization in mine tailings using nano-sized magnetite and zero valent iron with the enhancement of mobility by surface coating. *J. Geochem. Explor.* 113, 124–129. <https://doi.org/10.1016/j.gexplo.2011.07.002>.
- Klimkova, S., Cernik, M., Lacinova, L., Filip, J., Jancik, D., Zboril, R., 2011. Zero-valent iron nanoparticles in treatment of acid mine water from in situ uranium leaching. *Chemosphere* 82, 1178–1184. <https://doi.org/10.1016/j.chemosphere.2010.11.075>.
- Komárek, M., Vaněk, A., Ettler, V., 2013. Chemical stabilization of metals and arsenic in contaminated soils using oxides - a review. *Environ. Pollut.* <https://doi.org/10.1016/j.envpol.2012.07.045>.
- Kumpiene, J., Lagerkvist, A., Maurice, C., 2008. Stabilization of As, Cr, Cu, Pb and Zn in soil using amendments - a review. *Waste Manag.* 28, 215–225. <https://doi.org/10.1016/j.wasman.2006.12.012>.
- Lado, L.R., Hengli, T., Reuter, H.I., 2008. Heavy metals in European soils: a geo-statistical analysis of the FOREGS Geochemical database. *Geoderma* 148, 189–199. <https://doi.org/10.1016/j.geoderma.2008.09.020>.
- Laumann, S., Micić, V., Lowry, G.V., Hofmann, T., 2013. Carbonate minerals in porous media decrease mobility of polyacrylic acid modified zero-valent iron nanoparticles used for groundwater remediation. *Environ. Pollut.* 179, 53–60. <https://doi.org/10.1016/j.envpol.2013.04.004>.
- Li, Z., Greden, K., Alvarez, P.J.J., Gregory, K.B., Lowry, G.V., 2010. Adsorbed polymer and NOM limits adhesion and toxicity of nano scale zerovalent iron to *E. coli*. *Environ. Sci. Technol.* 44, 3462–3467. <https://doi.org/10.1021/es9031198>.
- Magiera, T., Zawadzki, J., Szuszkiewicz, M., Fabijańczyk, P., Steinnes, E., Fabian, K., Miszczak, E., 2018. Impact of an iron mine and a nickel smelter at the Norwegian-Russian border close to the Barents Sea on surface soil magnetic susceptibility and content of potentially toxic elements. *Chemosphere* 195, 48–62. <https://doi.org/10.1016/j.chemosphere.2017.12.060>.
- MAPA, 1994. *Métodos Oficiales de Análisis*, vol. III. Secretaría General Técnica Ministerio de Agricultura, Pesca y Alimentación, Madrid, pp. 219–324.
- Marker, B.R., 2018. *Brownfield Sites*, pp. 92–94. [https://doi.org/10.1007/978-3-319-73568-9\\_36](https://doi.org/10.1007/978-3-319-73568-9_36).
- Mesa, V., Navasas, A., González-Gil, R., González, A., Weyens, N., Lauga, B., Gallego, J.R., Sánchez, J., Peláez, A.I., 2017. Use of endophytic and rhizosphere bacteria to improve phytoremediation of arsenic-contaminated industrial soils by autochthonous *betula celtiberica*. *Appl. Environ. Microbiol.* 83. <https://doi.org/10.1128/aem.03411-16>.
- Mueller, N.C., Braun, J., Bruns, J., Černík, M., Rissing, P., Rickerby, D., Nowack, B., 2012. Application of nanoscale zero valent iron (nZVI) for groundwater remediation in Europe. *Environ. Sci. Pollut. Res.* 19, 550–558. <https://doi.org/10.1007/s11356-011-0576-3>.
- O'Carroll, D., Sleep, B., Krol, M., Boparai, H., Kocur, C., 2013. Nanoscale zero valent iron and bimetallic particles for contaminated site remediation. *Adv. Water Resour.* 51, 104–122. <https://doi.org/10.1016/j.advwatres.2012.02.005>.
- O'Reilly, S.E., Strawn, D.G., Sparks, D.L., 2010. Residence time effects on arsenate adsorption/desorption mechanisms on goethite. *Soil Sci. Soc. Am. J.* 65, 67. <https://doi.org/10.2136/sssaj2001.65167x>.
- Pérez-Sanz, A., Vázquez, S., Lobo, M.C., Moreno-Jimenez, E., García, P., Carpena, R.O., 2013. Soil Factor controlling arsenic availability for *Silene vulgaris*. *Commun. Soil*

- Sci. Plan. 44 (1414), 2152–2167. <https://doi.org/10.1080/00103624.2013.799683>.
- Rahimi, S., Moattari, R.M., Rajabi, L., Derakhshan, A.A., Keyhani, M., 2015. Iron oxide/hydroxide ( $\alpha,\gamma$ -FeOOH) nanoparticles as high potential adsorbents for lead removal from polluted aquatic media. *J. Ind. Eng. Chem.* 23, 33–43. <https://doi.org/10.1016/j.jiec.2014.07.039>.
- Rahmani, A.R., Ghaffari, H.R., Samadi, M.T., 2010. Removal of arsenic (III) from contaminated water by synthetic nano size zerovalent iron. *World Acad. Sci. Eng. Technol.* 4, 647–650.
- Ramos, M., Yan, W., Li, X., Koel, B., Zhang, W., 2009. Simultaneous oxidation and reduction of arsenic by zero-valent iron nanoparticles: understanding the significance of the core-shell structure. *J. Phys. Chem. C* 113 (33), 14591–14594. <https://doi.org/10.1021/jp9051837>.
- Rao, L.N., 2014. Environmental impact of uncontrolled disposal of e-wastes. *Int. J. Chem. Res.* 6, 1343–1353.
- Saccà, M.L., Fajardo, C., Costa, G., Lobo, C., Nande, M., Martin, M., 2014. Integrating classical and molecular approaches to evaluate the impact of nanosized zero-valent iron (nZVI) on soil organisms. *Chemosphere* 104, 184–189. <https://doi.org/10.1016/j.chemosphere.2013.11.013>.
- Santucci, L., Carol, E., Tanjal, C., 2018. Industrial waste as a source of surface and groundwater pollution for more than half a century in a sector of the Río de la Plata coastal plain (Argentina). *Chemosphere* 206, 727–735. <https://doi.org/10.1016/j.chemosphere.2018.05.084>.
- Schmid, D., Micić, V., Laumann, S., Hofmann, T., 2015. Measuring the reactivity of commercially available zero-valent iron nanoparticles used for environmental remediation with iopromide. *J. Contam. Hydrol.* 181, 36–45. <https://doi.org/10.1016/j.jconhyd.2015.01.006>.
- Siddiqui, S.I., Chaudhry, S.A., 2018. A review on graphene oxide and its composites preparation and their use for the removal of  $As^{3+}$  and  $As^{5+}$  from water under the effect of various parameters: application of isotherm, kinetic and thermodynamics. *Process Saf. Environ. Prot.* <https://doi.org/10.1016/j.psep.2018.07.020>.
- Singh, R., Misra, V., 2015. Stabilization of zero-valent iron nanoparticles: role of polymers and surfactants. In: *Handbook of Nanoparticles*. Springer. [https://doi.org/10.1007/978-3-319-13188-7\\_44-2](https://doi.org/10.1007/978-3-319-13188-7_44-2).
- Tessier, A., Campbell, P.G.C., Bisson, M., 1979. Sequential extraction procedure for the speciation of particulate trace metals. *Anal. Chem.* 51, 844–851. <https://doi.org/10.1021/ac50043a017>.
- Waychunas, G.A., Kim, C.S., Banfield, J.F., 2005. Nanoparticulate iron oxide minerals in soils and sediments: unique properties and contaminant scavenging mechanisms. *J. Nanoparticle Res.* 409–433. <https://doi.org/10.1007/s11051-005-6931-x>.
- Zhang, M.Y., Wang, Y., Zhao, D.Y., Pan, G., 2010. Immobilization of arsenic in soils by stabilized nanoscale zero-valent iron, iron sulfide (FeS), and magnetite ( $Fe_3O_4$ ) particles. *Chin. Sci. Bull.* 55, 365–372. <https://doi.org/10.1007/s11434-009-0703-4>.
- Zucconi, F., Monaco, A., Forte, M., De Bertoldi, M., 1985. Phytotoxins during the stabilization of organic matter. In: *Composting of Agricultural and Other Wastes*, pp. 73–86.